

FINITE ELEMENT MODELING OF FRICTION STIR WELDING IN ALUMINUM ALLOYS JOINT

Binnur Gören Kırıl^{1,*}, Mustafa Tabanoğlu², H. Tarık Serindağ²

¹ Dokuz Eylül University, Department of Mechanical Engineering, 35397, Tınaztepe, Izmir, Turkey

² Dokuz Eylül University, The Graduate School of Natural and Applied Sciences, Izmir, Turkey

binnur.goren@deu.edu.tr, mustafa_tabanoglu@yahoo.com, tarik.serindag@deu.edu.tr

Abstract - This study aims to model friction stir welding of the aluminum alloys using the finite element method. For this purpose, transient thermal finite element analyses are performed in order to obtain the temperature distribution in the welded aluminum plate during the welding operation. Heat input from the tool shoulder and the tool pin are considered in the finite element model. A moving heat source with a heat distribution simulating the heat generated from the friction between the tool shoulder and the work piece is used in the heat transfer analysis. Three-dimensional models are carried out by using ANSYS and HyperXtrude commercial softwares. APDL (ANSYS Parametric Design Language) code is developed to model moving heat source and change boundary conditions.

Key Words: Friction stir welding, Finite element analyses, Al6061, Transient thermal analysis.

1. INTRODUCTION

Friction stir welding (FSW) is a novel solid-state joining process that may have significant advantages compared to the fusion processes as follow: Joining of conventionally non-fusion weldable alloys, reduced distortion and improved mechanical properties of weldable alloys joints due to the pure solid-state joining of metals. In a typical FSW, a rotating cylindrical pin tool is forced to plunge into the plates to be welded and moved along their contact line. During the welding, heat is generated by contact friction between the tool and workpiece softens the material. Since no melting occurs during FSW, the process is performed at much lower temperatures than conventional welding techniques. Because of the highest temperature is lower than the melting temperature of the material, FSW yields fine microstructure [1].

Although it is a new welding technology, the FSW has been extensively studied both numerically and experimentally. Chen and Kovacevic studied on the finite element analysis of the thermal history and thermomechanical process in the butt-welding of aluminum alloy 6061- T6 [2]. Buffa *et al.* proposed a 3D FEM model for the FSW process that is thermo-mechanically coupled and with rigid-viscoplastic material behavior [3]. Nandan *et al.* modeled three-dimensional viscoplastic flow and temperature field during FSW of 304 austenitic stainless steel mathematically [4]. Chao *et al.* formulated the heat transfer of the FSW process into two boundary value problems (BVP)-a steady state BVP for the tool and a transient BVP for the workpiece.

They carried out the finite element analyses to determine the heat flux generated from the friction to the workpiece and the tool [5]. Zhang *et al.* developed solid mechanics-based finite element models and computational procedures to study the flow patterns and the residual stresses in FSW. They presented two-dimensional results of the material flow patterns and the residual stresses and investigated the flow of metal during FSW. They showed that the flows on the advancing side and retreating side are different. They investigated the residual stresses of the welded plate. They concluded that with the increase of the translational velocity, the maximum longitudinal residual stress can be increased [6]. Hamilton *et al.* developed a thermal model of FSW that utilizes a new slip factor based on the energy per unit length of weld. The slip factor was derived from an empirical, linear relationship observed between the ratio of the maximum welding temperature to the solidus temperature and the welding energy [7]. Song and Kovacevic presented a three-dimensional heat transfer model for FSW. They introduced a moving coordinate to reduce the difficulty of modeling the moving tool and considered heat input from the tool shoulder and the tool pin in their model. The finite difference method was applied in solving the control equations. They concluded that preheat to the workpiece is beneficial to FSW [8]. Rajamanickam *et al.* investigated the effect of process parameters such as tool rotation and weld speed on temperature distribution and mechanical properties of aluminum alloy AA2014 joined by friction stir welding. A three dimensional transient thermal model using finite element code ANSYS was developed and experimentally validated to quantify the thermal history [9]. Soundararajan *et al.* developed a thermo-mechanical model with both tool and workpiece using mechanical loading with thermal stress to predict the effective stress development at the bottom of workpiece with uniform boundary conditions. They used the stress to define the adaptable contact conductance values in the thermal model at the workpiece-backing plate interface and measured the temperatures at various locations during experiment using thermocouples to validate the finite element model predictions [10].

In the present study, the modeling of FSW process is carried out using the finite element method. Transient thermal finite element analyses are performed in order to obtain the temperature distribution in the welded aluminum plate during the welding operation. A moving heat source with a heat distribution simulating the heat generated from the friction between the tool shoulder and the work piece is used in the heat transfer analysis. Three-dimensional models are carried out by using ANSYS and HyperXtrude commercial softwares. APDL (ANSYS Parametric Design Language) code is developed to model moving heat source and change boundary conditions. The usage of APDL code removes the necessity of using ANSYS user interface. Advantage of ANSYS software is that the temperature outputs can be obtained at every desired time step.

2. HEAT GENERATION

Heat source during welding is considered as the friction between the rotating tool and the welded workpieces. The heat is generated at the interface of the tool shoulder and workpiece and tool pin and workpiece due to friction. The heat generated at the surface

of the tool is transferred into the tool following the Fourier's law of heat conduction [10]. The heat transfer equation for the tool in a static coordinate system is

$$\rho C_p \frac{\partial T}{\partial t} = \frac{\partial}{\partial x} \left(k_x \frac{\partial T}{\partial x} \right) + \frac{\partial}{\partial y} \left(k_y \frac{\partial T}{\partial y} \right) + \frac{\partial}{\partial z} \left(k_z \frac{\partial T}{\partial z} \right) \quad (1)$$

where T is the temperature, C_p is heat capacity, ρ is the density and k is the heat conductivity that varies with temperature in the calculations. The aluminum workpiece is an isotropic material properties, so that the identical value of thermal conductivity is used for all three directions.

Convection at the sides of the workpiece and tool is represented based on Newton's law of cooling as

$$k \frac{\partial T}{\partial n} = h(T - T_{amb}) \quad (2)$$

where T_{amb} is ambient temperature.

The torque required to rotate a circular shaft relative to the plate surface under the action of an axial load is given by [11]

$$\int_0^{M_R} dM = \int_0^R \mu P(r) 2\pi r^2 dr = \frac{2}{3} \mu \pi P R^3 \quad (3)$$

where M is the interfacial torque, μ is the friction coefficient, R is the surface radius, and $P(r)$ is the pressure distribution across the interface. If all the shearing work at the interface is converted into frictional heat, the average heat input per unit area and time becomes

$$Q_1 = \int_0^{M_R} \omega dM = \int_0^R \omega \mu P(r) 2\pi r^2 dr \quad (4)$$

where Q_1 is the net power [W], ω is the angular velocity [rad/s] and P is the pressure [MPa]. The pressure P cannot exceed the actual flow stress of the material at the operating temperature [11]. Q_1 is the heat generated by the shoulder.

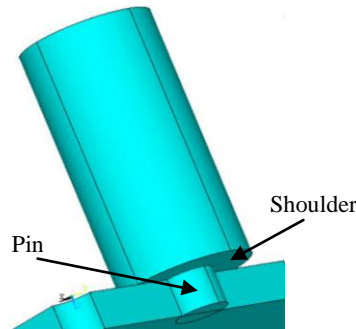


Figure 1. Three-dimensional model of the friction stir welding process.

Heat input depends both on rotational speed and the shoulder radius. These parameters are the main process variables in friction stir processing. The ratio of heat generated from the pin, Q_2 and the heat generated from the shoulder, Q_1 is 0.128 [11, 12].

The initial temperature of the workpiece is assumed to be equal to the ambient temperature (25°C). A convection coefficient of 30 W/m² °C is applied at the top and side surfaces of the workpiece. Since the value of conductive coefficient between the workpiece and the backing plate is not known, convective coefficient of 300 W/m² °C is applied to the bottom surface of the work piece [11].

3. FINITE ELEMENT ANALYSES

3.1. Modeling

Two 6061-T6 Al alloy plates, each with a dimension of 150 × 200 × 3.1 mm are butt welded in the adapted vertical milling machine for FSW when HyperXtrude program is used. Because of the symmetry only one plate is modeled in ANSYS program. In the present thermal analysis, the workpiece is meshed using a brick element called SOLID70 when ANSYS software is used. This element has a three-dimension thermal conduction capability and can be used for a three-dimensional, steady-state or transient thermal analysis. The element is defined by eight nodes with temperature as single degree of freedom at each node and by the orthotropic material properties [13]. An advantage of using this element is that, the element can be replaced by an equivalent structural element for the structural analysis. Figure 2 shows the finite element model of the aluminum workpiece generated by ANSYS software. For the finite element analyses by ANSYS, APDL (ANSYS parametric design language) is used to develop a subroutine for a transient moving heat source model. Transient finite element analyses are performed considering moving heat source.

Results obtained using ANSYS are compared to the results obtained using Friction Stir Welding Module of HyperXtrude software. Figure 3 shows the modeling of FSW carried out using HyperXtrude software.

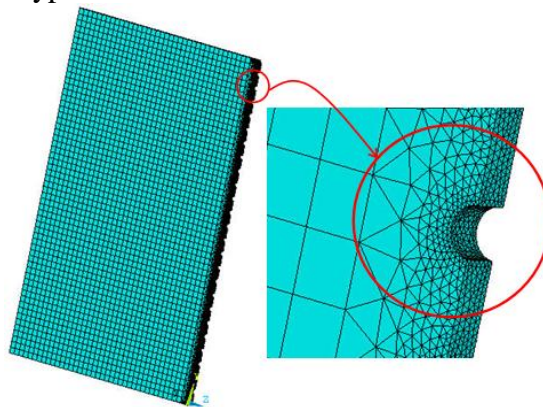


Figure 2. Finite element model of the aluminum workpiece by ANSYS software.

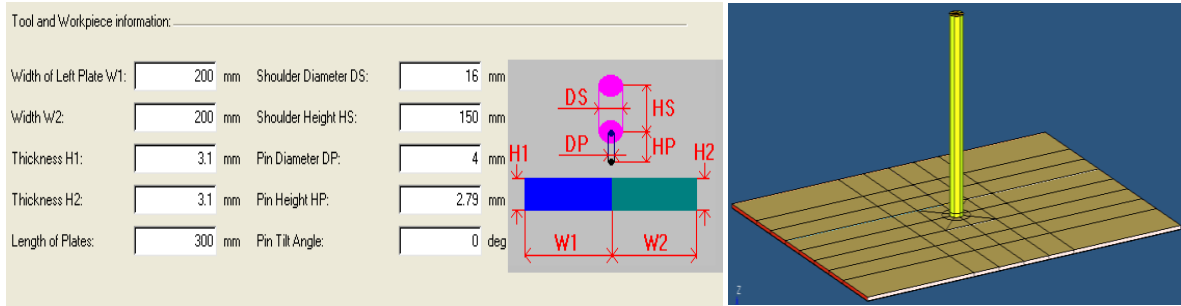


Figure 3. Modeling of FSW by HyperXtrude software.

3.2. Defining of Material Properties and Boundary Conditions

Thermal conductivity, k and heat capacity, C_p are dependent on temperature. Table 1 presents the variation of material properties of AA6061-T6 with respect to temperature used in the finite element analyses.

Table 1. Variation of material properties of AA6061-T6 with respect to temperature.

| T (°C) | k (W/m °C) | C_p (J/kg °C) |
|--------|--------------|-----------------|
| -17.8 | 162 | 904 |
| 37.8 | 162 | 945 |
| 93.3 | 177 | 978 |
| 148.9 | 184 | 1004 |
| 204.4 | 192 | 1028 |
| 260 | 201 | 1052 |
| 315.6 | 207 | 1078 |
| 371.1 | 217 | 1104 |
| 426.7 | 223 | 1133 |
| 571.1 | 253 | 1230 |

Figure 4 presents the boundary conditions of FSW process modeled. As seen from the figure, heat flux is applied on the interface of tool shoulder and pin and workpiece. Convection coefficients of $30 \text{ W/m}^2 \text{ °C}$ and $300 \text{ W/m}^2 \text{ °C}$ are applied at the top and side surfaces of the work piece and to the bottom surface of the workpiece, respectively.

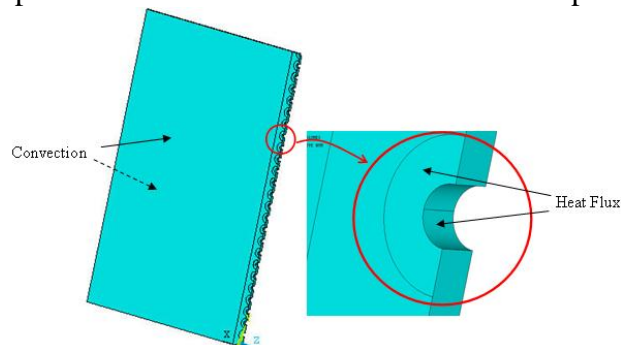


Figure 4. Boundary conditions.

The flowchart for transient thermal analysis is shown in Figure 5.

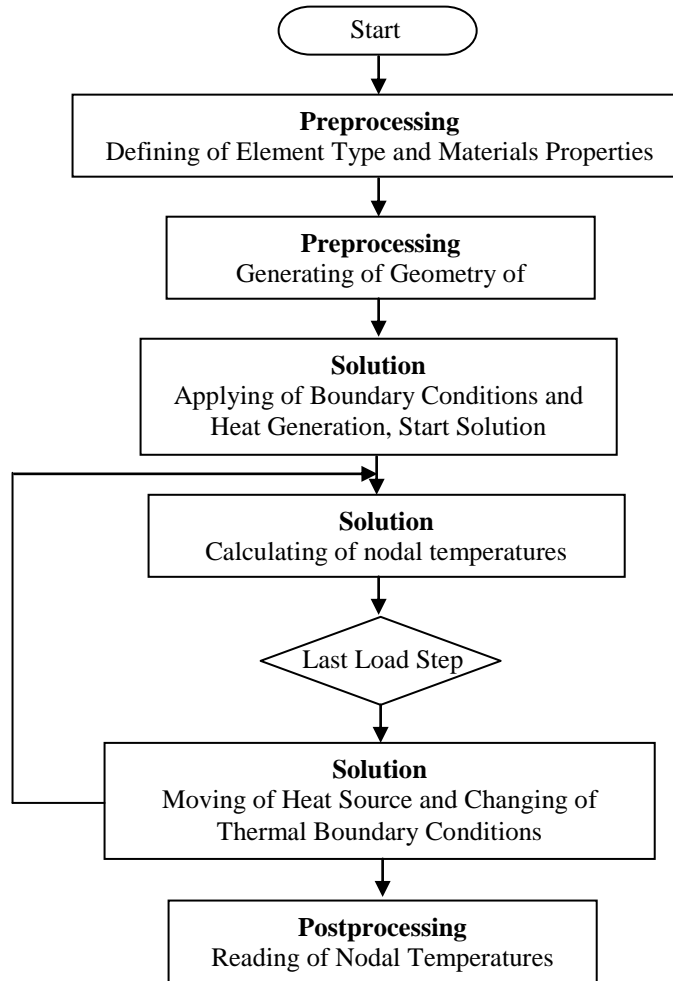


Figure 5. Flowchart for transient thermal finite element analysis

4. RESULTS

In the present study, the modeling of friction stir welding is carried out using both ANSYS and HyperXtrude commercial softwares. APDL (ANSYS Parametric Design Language) code is developed for transient thermal analyses. Transient thermal finite element analyses are performed in order to obtain the temperature distribution in the welded aluminum plates during the welding operation.

Figures 4 and 5 show the temperature profiles in the workpiece during the welding operation for $\omega=800$ rev/min, $v=2.5$ mm/s and $v=5$ mm/s. As seen from the figures, temperature values obtained by ANSYS and HyperXtrude agree with each other.

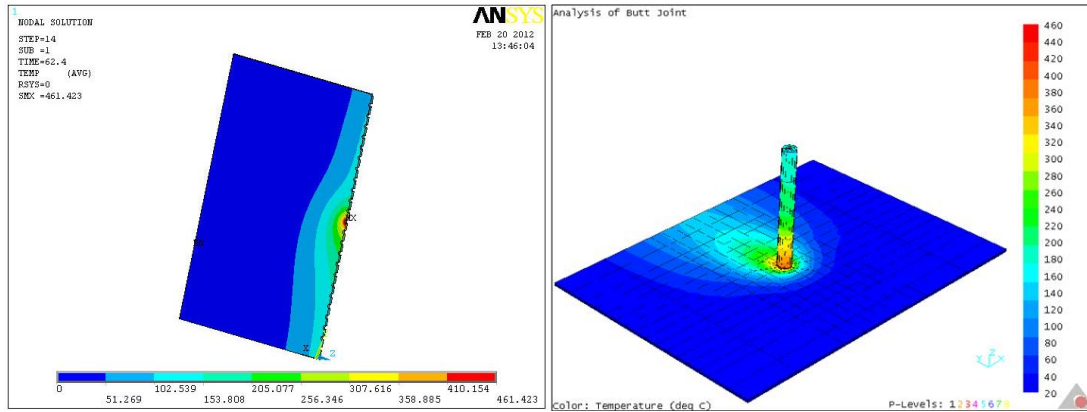


Figure 4. Temperature distributions obtained (a) by ANSYS (b) HyperXtrude softwares in welded AA 6061-T6 plates for $\omega=800$ rev/min and $v= 2.5$ mm/s.

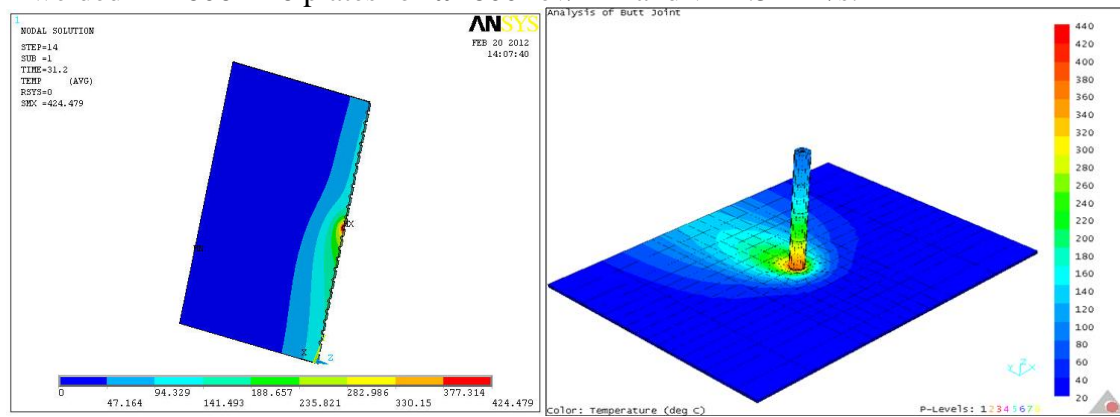


Figure 5. Temperature distributions obtained (a) by ANSYS (b) HyperXtrude softwares in welded AA 6061-T6 plates for $\omega=800$ rev/min and $v= 5$ mm/s.

The input welding parameters used in the finite element calculations are presented in Table 2.

Table 2. Input welding parameters.

| | A | B | C | D | E | F |
|-----------------------------------|-----|------|------|-----|------|------|
| Rotational speed (rev/min) | 800 | 1000 | 1200 | 800 | 1000 | 1200 |
| Transverse speed (mm/s) | 2.5 | 2.5 | 2.5 | 5 | 5 | 5 |

Table 3. Temperature values obtained by HyperXtrude software.

| | Rotational speed (rev/min) | Transverse speed (mm/s) | Temperature (°C) |
|----------|-----------------------------------|--------------------------------|-------------------------|
| A | 800 | 2.5 | 440.355 |
| B | 1000 | 2.5 | 460.778 |
| C | 1200 | 2.5 | 484.401 |
| D | 800 | 5 | 430.572 |
| E | 1000 | 5 | 452.443 |
| F | 1200 | 5 | 478.449 |

Table 3 shows the maximum temperatures obtained by finite element analyses using HyperXtrude software. The transverse speeds considered are 2.5 and 5 mm/s while the tool rotational speeds are 800, 1000 and 1200 rev/min. As seen from the table, temperature during the welding increases as the rotational speed increases and the transverse speed decreases.

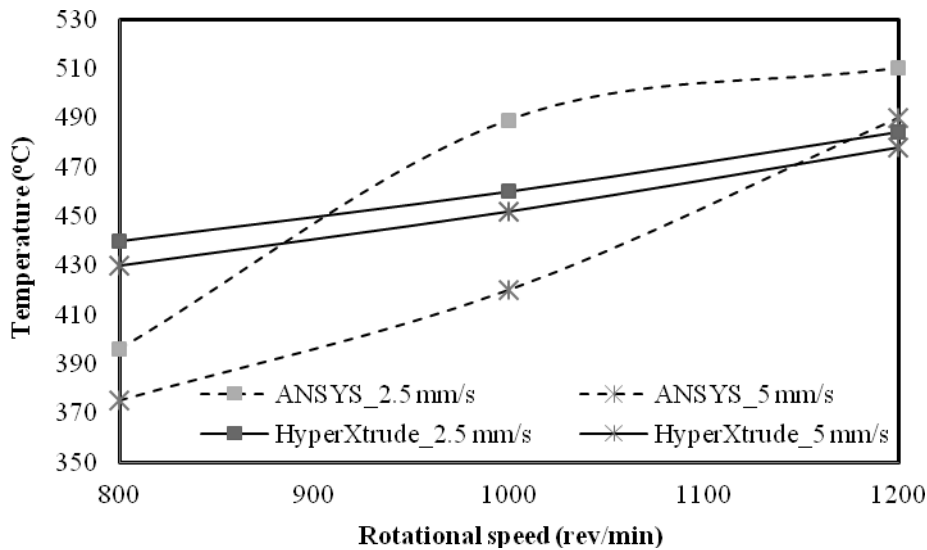


Figure 6. Comparison of results obtained by ANSYS and HyperXtrude.

Figure 6 shows the comparison of the maximum temperature occurred during friction stir welding modeled by ANSYS and HyperXtrude. As seen from the figure, the maximum temperature increases gradually as the rotational speed increases and transverse speed decreases when HyperXtrude software is used. Dotted lines show the results obtained running APDL code developed in ANSYS software. The differences between the results stem from the mathematical models used in the softwares.

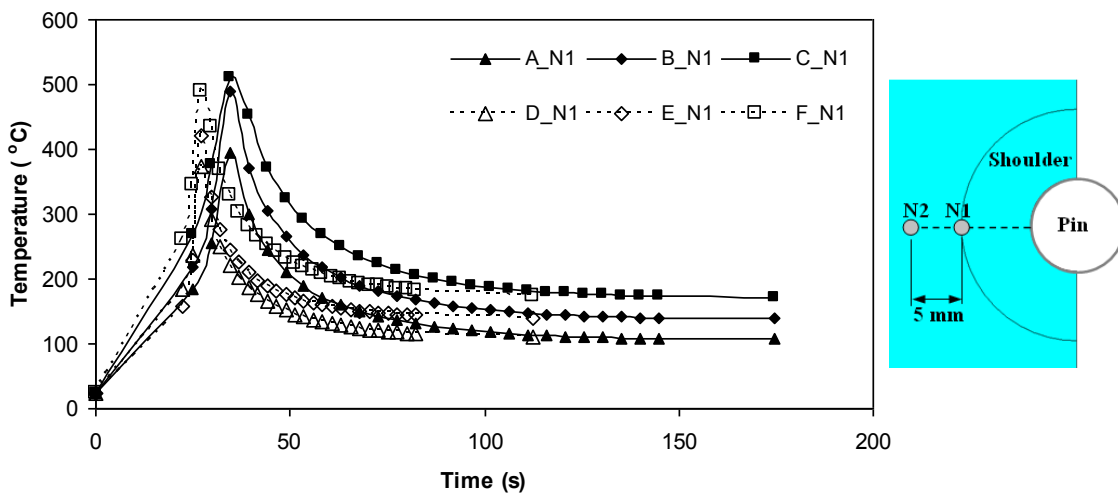


Figure 7. Temperature–time profile for location N1.

Figures 7 and 8 show the transient temperatures from the numerical calculations carried out using ANSYS for locations N1 and N2. As seen from the figures, temperature increases while the rotational speed of the tool increases and transverse speed decreases. The maximum temperatures obtained from the numerical analyses near the weld are higher than recrystallizing temperature of the aluminum.

The relation between tool holding time and temperature during FSW process is shown in Figure 9. As seen from the figure, as the tool holding time is increased, the maximum temperature near the weld increases. The increase of this processing parameter results in more extensive stirring or sufficient heat input during the FSW process. The weld microstructures vary significantly depending on tool holding time as well as tool rotational and transverse speeds.

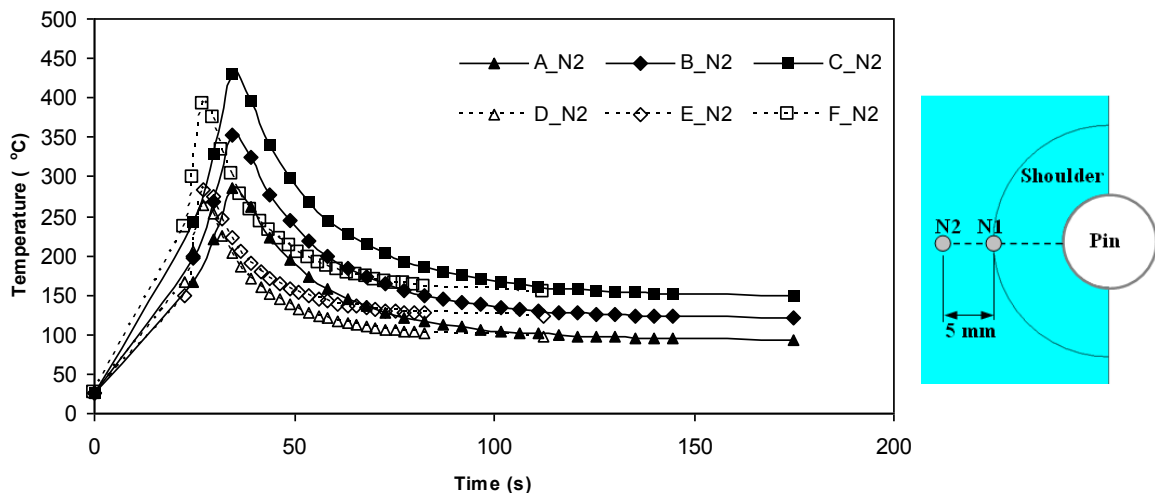


Figure 8. Temperature–time profile for location N2.

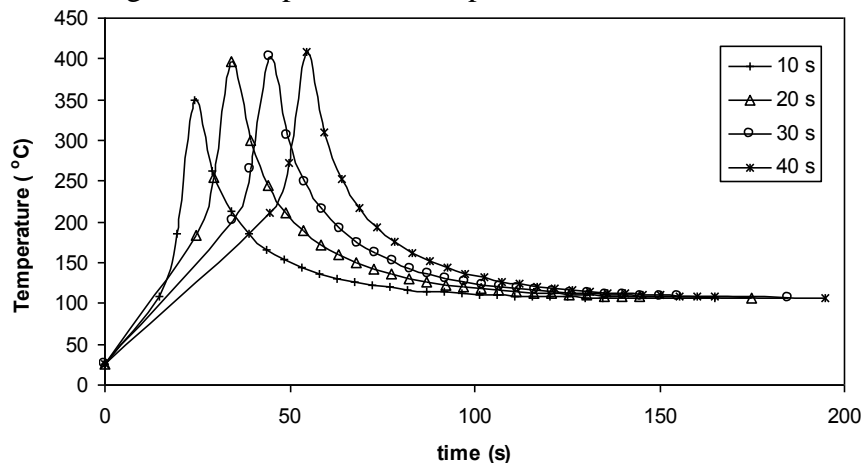


Figure 9. Temperature–time profile for location N1 with respect to holding time.

5. CONCLUDING REMARKS

In the present study, the modeling of friction stir welding is carried out using the transient finite element analyses. A moving heat source with a heat distribution simulating the heat generated from the friction between the tool shoulder and the

workpiece is used in the heat transfer analysis. It is observed that the maximum temperature near the weld increases as the tool holding time and rotational speed are increased. Temperature decreases as the tool transverse speed increases. Additionally, it can be concluded that use of a moving heat source technique is proved to be a reliable method to simulate friction stir processing.

Acknowledgement- Authors wish to thank TIRSAN Kardan Inc. for invaluable helps in the use of HyperXtrude Software.

6. REFERENCES

1. M.B. Bilgin, C. Meran, The effect of tool rotational and traverse speed on friction stir weldability of AISI 430 ferritic stainless steels, *Materials&Design* **33**, 376–383, 2012.
2. C.M. Chen, R. Kovacevic, Finite element modeling of friction stir welding-thermal and thermomechanical analysis, *International Journal of Machine Tools & Manufacture* **43**, 1319–1326, 2003.
3. G. Buffa, J. Hua, R. Shivpuri, L. Fratini, A continuum based fem model for friction stir welding—model development, *Materials Science and Engineering A* **419** 389–396, 2006.
4. R. Nandan, G.G. Roy, T. J. Lienert and T. DebRoy, Numerical modelling of 3D plastic flow and heat transfer during friction stir welding of stainless steel, *Science and Technology of Welding and Joining* **11**, 5 52-537, 2006.
5. Y.J. Chao, X. Qi, W. Tang, Heat transfer in friction stir welding-Experimental and numerical studies, *Transactions of the ASME* **125**, 138-145, 2003.
6. H.W. Zhang, Z.Zhang, J.T.Chen, The finite element simulation of the friction stir welding process. *Materials Science and Engineering A* **403**, 340–348, 2005.
7. C. Hamilton, S. Dymek, A. Sommers (2008) A thermal model of friction stir welding in aluminum alloys, *International Journal of Machine Tools & Manufacture* **48**, 1120–1130, 2008.
8. M. Song, R. Kovacevic, Thermal modeling of friction stir welding in a moving coordinate system and its validation, *International Journal of Machine Tools & Manufacture* **43**, 605–615, 2003.
9. N. Rajamanickam, V.Balusamy, G.Madhusudhanna Reddy, K.Natarajan, Effect of process parameters on thermal history and mechanical properties of friction stir welds, *Materials&Design* **30** 2726–2731, 2009.
10. V. Soundararajan, S. Zekovic, R. Kovacevic, Thermo-mechanical model with adaptive boundary conditions for friction stir welding of Al 6061, *International Journal of Machine Tools & Manufacture* **45** 1577–1587, 2005.
11. K.H. Vepakomma, Three dimensional thermal modeling of friction stir processing MSc Thesis, The Florida State University College of Engineering, 2006.
12. H. Schmidt, J. Hattel, J. Wert, An Analytical Model for the Heat Generation in Friction Stir Welding, *Modelling and Simulation in Material Science Engineering* **12** 143–157, 2004.
13. ANSYS 10.0 Documentation.